Heliyon 10 (2024) e30786

Contents lists available at ScienceDirect

Heliyon

journal homepage: www.cell.com/heliyon

Research article

Resveratrol protects against diabetic retinal ganglion cell damage by activating the Nrf2 signaling pathway

Dongqing Yuan [a,1], Yingnan Xu [b,1], Lian Xue [c], Weiwei Zhang [a], Liuwei Gu [a], Qinghuai Liu [a,*]

[a] Department of Ophthalmology, Jiangsu Province Hospital, The First Affiliated Hospital with Nanjing Medical University, Jiangsu Women and Children Health Hospital, 300 Guangzhou Road, Nanjing, Jiangsu, 210029, China
[b] Department of Ophthalmology, The Affiliated Eye Hospital of Nanjing Medical University, Nanjing, China
[c] Department of Neurology, Affiliated Hospital of Integrated Traditional Chinese and Western Medicine, Nanjing University of Chinese Medicine, Jiangsu Province Academy of Traditional Chinese Medicine, Nanjing, China

ARTICLE INFO

Keywords:
Resveratrol
Diabetic retinopathy
Oxidative stress
Retinal ganglion cells
Apoptosis
Nrf2/HO-1 pathway

ABSTRACT

Objective: Oxidative stress-induced retinal neurodegenerative changes are among the pathological alterations observed in diabetic retinopathy. Resveratrol (RSV), a polyphenolic compound with diverse pharmacological effects, has shown preventive qualities in several neurodegenerative illnesses, including anti-inflammatory, anti-aging, and antioxidant benefits. However, its therapeutic efficacy in diabetic retinal neurodegeneration has not yet been thoroughly elucidated. Our study aimed to explore the protective mechanisms and therapeutic benefits of RSV on diabetic retinal neurodegeneration alterations.

Materials and methods: Using streptozotocin, we created a diabetic mouse model and conducted visual electrophysiological examinations on mice from the normal group, diabetic group, and diabetic group treated with RSV. Retinas were harvested for histological staining. Additionally, primary retinal ganglion cells cultured in high glucose conditions were used to assess malondialdehyde (MDA) levels and superoxide dismutase (SOD) levels upon siRNA-mediated nuclear factor erythroid 2-related factor 2 (Nrf2) interference. Protein levels of Nrf-2, heme oxygenase-1 (HO-1), and transcriptional levels of them were also measured.

Results: We demonstrated that RSV significantly improved the retinal morphology and function in the diabetic retinopathy model mice. The treated mice exhibited notable improvements in visual electrophysiology, with a significant reduction in retinal ganglion cell apoptosis. Following RSV treatment, the high glucose-cultured ganglion cells demonstrated a considerable rise in SOD levels and a substantial drop in MOD. Moreover, the protein expression of solute carrier family 7 member 11 (SLC7A11) and Nrf2 significantly increased. RT-PCR and Western blot results indicated a significant attenuation of RSV's therapeutic effects upon Nrf2 inhibition.

Conclusion: Our findings suggest that RSV may reduce oxidative stress levels in the retina and inhibit retinal ganglion cell apoptosis via reducing the Nrf2/HO-1 pathway, which lessens the harm that excessive glucose causes to the retina.

* Corresponding author.
E-mail addresses: wuyuleng@126.com (D. Yuan), xyn20051151187@163.com (Y. Xu), 275204751@qq.com (L. Xue), zhang_weiwei@139.com (W. Zhang), Glw0115@126.com (L. Gu), liuqh@njmu.edu.cn (Q. Liu).
[1] These two authors contributed equally to the article.

https://doi.org/10.1016/j.heliyon.2024.e30786
Received 21 February 2024; Received in revised form 5 May 2024; Accepted 6 May 2024
Available online 6 May 2024

1. Introduction

Diabetic Retinopathy (DR) is a major complication in diabetic patients, characterized by increased inflammatory responses, ischemia, progressive retinal pigment epithelium (RPE) cells transformation leading to retinal blood barrier dysfunction, and blindness [1]. In recent years, with the progression of diabetes, the incidence of complications has increased. As of 2015, there were approximately 400 million cases of type 2 diabetes worldwide, with over 45% of individuals suffering from DR, making it a leading cause of acquired blindness globally [2]. By 2030, it is estimated that the global DR patient population will rise to 191 million, with 56.3 million individuals facing vision threats. The pathogenesis of DR is complex, with oxidative stress closely associated with its development [3]. Hyperglycemia induces metabolic abnormalities in the retina, resulting in the generation of reactive oxygen species (ROS). Oxidative stress, a key process in the development of DR, can be triggered by excessive ROS [4]. Typically, oxidative stress leads to dysfunction of endothelial cells, impaired blood vessel formation, and localized cell apoptosis, promoting the occurrence of retinal lesions. The current clinical treatments for DR primarily involve laser photocoagulation and vitrectomy, which may cause some damage to patients' vision [5]. Various chemotherapeutic drugs are still in the experimental or preclinical stages, with anti-VEGF drugs being relatively successful but effective only for proliferative DR, not for non-proliferative DR [6]. Therefore, the search for and development of suitable natural antioxidants to reduce the production of ROS and free radicals may have a protective effect on DR.

Resveratrol (RSV) is a non-flavonoid polyphenolic molecule which presents in many plants, such as grapes, peanuts, mulberries, and Japanese knotweed [7]. RSV possesses potent pharmacological effects, including as anti-aging, anti-thrombotic, antioxidant, and cardioprotective qualities [8]. It is distinguished by its low adverse effects, extensive availability, cost-effectiveness, and great biological safety. Studies indicate that RSV, as a hydrophilic small molecule, can penetrate the blood retinal barrier (BRB) [9,10]. RSV is essential for treating ocular disorders and associated repercussions through a number of mechanisms, such as oxidative stress, inflammation, apoptosis, mitochondrial malfunction, survival promotion, and stimulation of angiogenesis. A study on streptozotocin (STZ)-induced diabetic rats and diabetic retinopathy donor samples further confirmed that Alterations to the Nrf2-Keap1 pathway might be a possible supplementary treatment to manage oxidative stress and prevent the progression of diabetic retinopathy [11,12]. In comparison to wild-type mice, diabetic mice with Nrf2 gene knockout exhibited a significant increase in ROS and the inflammatory factor TNF-α in the retina, along with reduced expression of glutathione, indicating earlier impairment of BRB and neuronal dysfunction. RSV has been proven to activate the Nrf2 pathway, preventing cerebral ischemia-induced brain damage [13]. Therefore, we speculate whether RSV prevents diabetic retinal neuropathy via boosting Nrf2 transcriptional activity and expression. Therefore, the purpose of this study is to investigate the preventive effects of RSV on retinal ganglion cells and its associated signaling pathways by inducing a mouse model of diabetic retinal neuropathy.

2. Materials and Methods

2.1. Animals

8-week-old male C57BL6 mice with a body weight of approximately 25–30g were used as experimental subjects and were obtained from the Nanjing University Laboratory Animal Center. The mice were kept in an environment with a 12-h light-dark cycle and a regulated temperature of around 24 °C in the Clinical Research Center of Nanjing Medical University 's animal barrier system. Prior to each experiment, all mice were acclimated to these conditions through adaptive feeding for one week. Subsequently, the mice were randomized into four groups: one for control, one for STZ-induced diabetic mellitus (DM) and one for DM with RSV. The control group received RSV treatment. STZ (50 mg/kg; Sigma, USA) was injected intraperitoneally for five days to develop diabetes mellitus. Random blood glucose readings higher than 16.7 mmol/L one week following the previous STZ injection demonstrated the effective formation of the mouse diabetes model. The administration of resveratrol (Sigma, USA) involved oral gavage at a dosage of 10 mg/kg/day, with the treatment duration spanning one month. The Institutional Animal Research Committee of Nanjing Medical University granted approval for all animal research (No: 20,210,132).

2.2. Cell isolation and culture

From C57BL/6 mouse pups that were between 0 and 3 postnatal days old, primary retinal ganglion cells (RGCs) were extracted. For 15 min, the extracted retinas were separated using a collagenase solution (70 units/ml) and a papain solution (15 units/ml). The retinal cell suspensions were treated with antimacrophage serum (1:100) for 1 h at 37 °C in order to eradicate macrophages and microglial cells. After that, the non-adherent cells were moved to 100 mm petri plates that had already been coated with anti-Thy1.2 antibody in order to purify RGCs for a duration of 1 h at 37 °C. The plates were then cleaned with PBS to get rid of the non-adherent cells. Adherent RGCs were removed off the plate by incubating with 0.025% trypsin for 5 min at 37 °C after being rinsed in panning buffer (Dulbecco's-PBS, 0.02% bovine serum albumin, 5 mg/mL insulin). The cells were then planted at a density of $2.03 \times 10\hat{}5$ cells/well. A glucose concentration of 5 mM (control) or 25 mM (high glucose, HG) was achieved in the cell growth media by modifying it once the density of the cells approached 50%–60%. Except in cases where otherwise noted, RSV was added to reach a concentration of 10 nM. After being incubated for 24 h, the cells were either lysed or fixed.

2.3. Electroretinography measurement

The recording instrument used was the RETLport visual physiology detection system (Roland, Germany), with a DELL color display screen measuring 40cm × 30 cm. The stimulation method employed a horizontal bar grid, with the corneal vertex positioned 15 cm from the center of the stimulus field, overlaid 200 times. The recording time was set at 200 ms, and the resistance during recording was ensured to be below 10 kΩ. After applying artificial tears to the examined eye, it was fixed at the corneal margin. On the same side of the studied eye, the ground electrode and reference electrode were positioned beneath the skin in the tail and cheek areas, respectively. The mouse's position was adjusted to align the visual axis of the examined eye vertically with the stimulus screen. The RETLport software was used to measure the N-P wave amplitude and implicit time of the mice's Pattern Electroretinography (ERG).

2.4. TUNEL staining

The eyeballs from each group were extracted, and after removing the cornea and lenses, they were left for 2 h in 4% paraformaldehyde. The specimens were then embedded in Tissue-Tek OCT compound after being dried in solutions containing 20–30% sucrose. Snap-freezing was done at −80 °C, and 10 μm sections were obtained. The Fluorescein in Situ Cell Death Detection Kit (Promega, USA) was then used to perform TUNEL staining in accordance with the manufacturer's instructions for experimental protocols.

2.5. Immunofluorescent staining for Nrf2 and SLC7A11 in retina

The sections were blocked with 5% BSA for 1 h, and then the primary antibody was incubated at 4 °C for the whole night. The thin pieces were incubated for 5 min apiece, and then they were rinsed three times in PBS. The slices were then left to incubate for 2 h at room temperature with the fluorophore-conjugated secondary antibody. Subsequently, the slices were examined using a Leica Thunder (German) fluorescent microscope after being counterstained with DAPI.

2.6. Oxidative stress measurement

Using commercial kits and following the manufacturer's instructions, the activity levels of superoxide dismutase (SOD, A001-3-2) and malondialdehyde (MDA, A003-4-1) in RGCs were measured (Nanjing Aiberg Biotechnology Co., Ltd., China). The homogenized cell samples were centrifuged at 13,000 rpm/min for 15 min at 4 °C to get the supernatant after they had been crushed with an ultrasonic crusher. According to the instructions, the pertinent chemicals were thereafter added and mixed with the supernatant. From a detection principle perspective, the interaction between MDA and thiobarbituric acid resulted in a red hue and the measurement of absorbance at 532 nm. The superoxide anion radical converted nitroblue tetrazolium to a blue mean product, which was not removed by SOD, and the absorbance at 450 nm was noted. A protein test kit containing bicinchoninic acid was used to measure the protein content.

2.7. RNA interference

Following the manufacturer's instructions, RGCs were transfected for 48 h with RNA interference targeting Nrf2 fragments that were bought from Gene Pharma Biotechnology using Lipofectamine 2000 reagent (11,668,019, Invitrogen, USA). For further tests, the siRNA fragments that exhibited the best effectiveness were chosen based on their Western blot detection results. Table 1 contains a list of all the siRNA primer sequences that were employed.

2.8. Real-time qRT-PCR with RNA extraction

RGCs were treated with Trizol reagent (Invitrogen, USA) to extract total RNA. Using a Reverse Transcription Kit (RR036A, Takara Biotechnology, Japan) and following the manufacturer's instructions, 1 μg of total RNA was used to create the first-strand cDNA. An apparatus made by Bio-Rad Laboratories called qRT-PCR was used to assess the expressions of genes linked to oxidative stress. The internal control for the amounts of mRNA expression was β-actin. The relative mRNA expression was determined using the $2-\Delta\Delta CT$

Table 1
The siRNA sequences of Nrf2.

Gene Names	Sequence (5' → 3')
scrambled siRNA	UUCUCCGAACGUGUCACGUTT
	ACGUGACACGUUCGGAGAATT
siNrf2-1	GGGAGGAGCUAUUAUCCAUTT
	AUGGAUAAUAGCUCCUCCCTT
siNrf2-2	CCUGAAAGCACAGCAGAAUTT
	AUUCUGCUGUGCUUUCAGGTT
siNrf2-3	CCUGCUACUUUAAGCCAUUTT
	AAUGGCUUAAAGUAGCAGGTT

technique (Livak and Schmittgen, 2001). Table 2 contains a list of all primer sequences that were employed.

2.9. Western blot analysis

Protease inhibitor-containing Radio Immunoprecipitation Assay lysis buffer (P0013B, Beyotime, China) was used to lyse the RGCs, and it was left on ice for 30 min. The supernatants were collected and the protein content was measured using a BCA Protein Assay kit following a 15-min centrifugation by 12,000 rpm/mim. Following their separation by electrophoresis on a 12% SDS-PAGE, the proteins were placed onto PVDF (polyvinylidene fluoride) membranes from Millipore, USA. The main antibody was blocked with 5% non-fat milk and then incubated at 4 °C for a whole night. After three rounds of washing with We used TBST (Tris-buffered saline containing Tween) to wash for three rounds, and added HRP-labeled secondary antibodies (1:7000) with a 2-h incubation period. The protein expression was then seen using an improved chemiluminescence detection kit (P0018AM, Beyotime, China) with β-actin serving as an internal reference. Optical density was used to quantify the relative intensity of the protein bands using ImageJ software 8.0 (NIH, Bethesda, MD, USA).

2.10. Statistical analysis

Software from GraphPad Prism 9.0 (San Diego, CA, USA) was used to analyze all of the data. Prior to statistical analysis, normality checks were performed, and the findings were shown as means ± standard deviation (SD). To compare two groups, the Student's t-test was employed. The nonparametric Mann-Whitney test was used after the Kruskal-Wallis test for multiple-group comparisons. Any change that was deemed statistically significant had a p-value of less than 0.05.

3. Results

3.1. Histopathological evaluation

We collected mouse retinas from different groups for H&E staining to observe the morphology of retinal tissue, particularly the morphology of ganglion cells, in order to investigate the protective effect of RSV on the optic nerve. As illustrated in Fig. 1A, the retinal structure of normal mice exhibited clear organization in all layers, with a normal density of ganglion cells and no apparent vacuoles between cells. In the DM model group, a reduction in retinal thickness compared to the control group was observed, along with a significant decrease in the density of ganglion cells (Fig. 1B–E). The cells appeared discontinuous, and some vacuoles were present. Although the structure of the retinal tissue in the RSV therapy group did not approach the level of the normal group, we did see a considerable improvement over the model group. The number of ganglion cells was much higher than in the model group.

3.2. Protective effect of RSV on retinal function in diabetic mice

Fig. 2A displays the results of pattern ERG implicit time and amplitude measurements in mice retinas after one month of treatment. In the retinas of normal mice, the P50 wave had an average amplitude of 5.69 ± 0.37 Mv (Fig. 2B) and an implicit duration of roughly 86.97 ± 3.02 ms (Fig. 2E). Furthermore, the N95 wave had an average amplitude of 8.35 ± 0.40 Mv (Fig. 2C) and an implicit duration of about 126.41 ± 5.57 ms (Fig. 2F). We also used N95/P50 amplitude to avoid issues arising from comparing N95 wave amplitudes when they are too small or absent (Fig. 2D). In the diabetic mouse model, we observed that the P50 and N95 waves had implicit timings and average amplitudes that were comparable to those of the normal group. In the retinas of mice treated with RSV, these values changed to 4.44 ± 0.41 mV for the P50 wave amplitude, 100.18 ± 3.60 ms for the P50 wave implicit time, 5.93 ± 0.40 mV for the N95 wave amplitude, and 149.78 ± 5.09 ms for the N95 wave implicit time. For the group receiving RSV alone, these values changed to 3.02 ± 0.42 mV for the P50 wave amplitude, 115.58 ± 7.59 ms for the P50 wave implicit time, 4.43 ± 0.42 mV for the N95 wave amplitude, and 174.46 ± 5.41 ms for the N95 wave implicit time. The diabetes group of mice had considerably lower and delayed implicit timings and amplitudes of the P50 and N95 waves in comparison to the non-diabetic control group ($P < 0.001$ and $P < 0.01$, respectively). On the other hand, compared to the model group, the implicit timings and amplitudes of the P50 and N95 waves showed a considerable improvement after one month of RSV therapy ($P < 0.001$ and $P < 0.01$, respectively).

Table 2
Sequences of oligonucleotide primers for qRT-PCR.

Gene Names	primer	Sequence (5' → 3')	length (bp)	Species
Nrf2	Forward	TACTCCCAGGTTGCCCACA	19	Mouse
	Reverse	CATCTACAAACGGGAATGTCTGC	23	
HO-1	Forward	CACGCATATACCCGCTACCT	19	Mouse
	Reverse	CCAGAGTGTTCATTCGAGCA	20	
β-actin	Forward	TCAGGTCATCACTATCGGCAAT	22	Mouse
	Reverse	AAGAAAGGGTGTAAAACGCA	20	

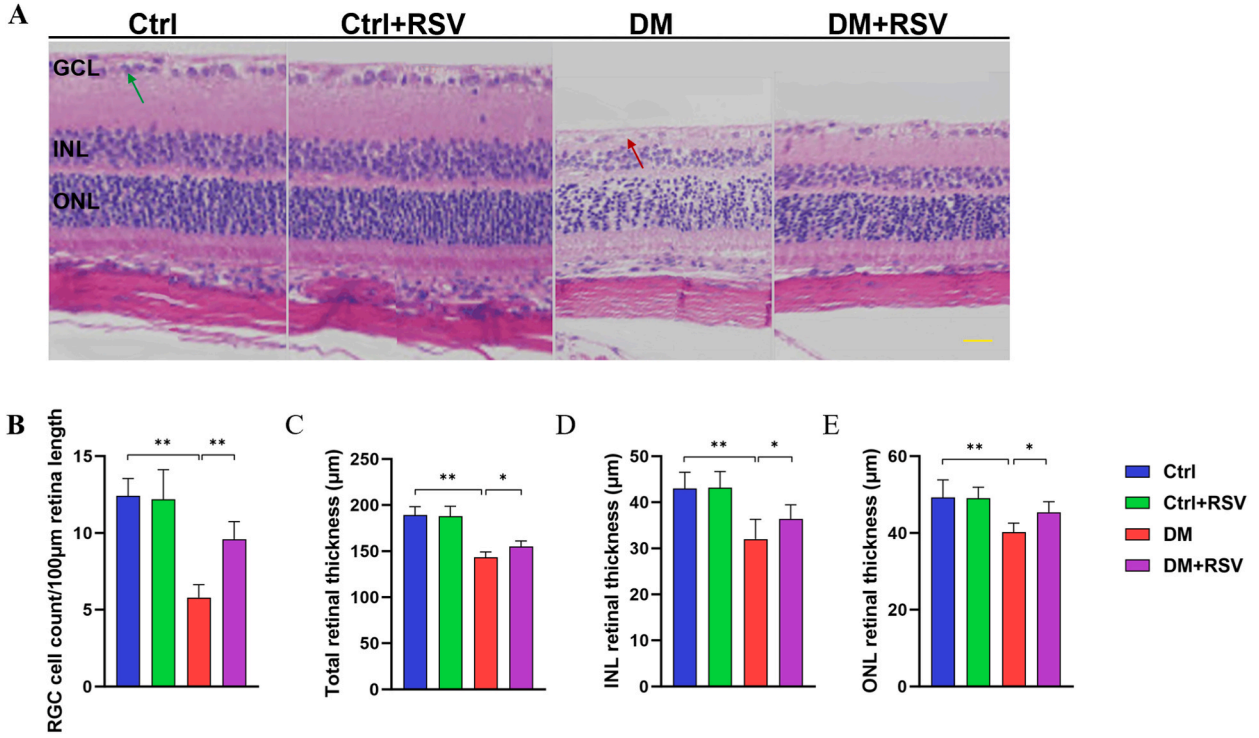

Fig. 1. The retinal tissue morphology for H&E staining in various groups. (A) The retinal structure changed in DM model compared with Ctrl. Scale bar: 100 μm. The green arrows indicate normal RGCs, while the red arrows indicate RGCs in DM. (B) RGC cell count in retina in different groups, and the RGC cells was significantly decreased in DM model, whereas increased in DM + RSV group. (C) The thickness of total retina in different groups. (D) The INL thickness in different groups. (E) The ONL thickness in different groups. The data is displayed as Mean ± SD. A multiple-group comparison (n = 5) was conducted using the nonparametric Kruskal-Wallis test and the Mann-Whitney test after that. GCL: Ganglion Cell Layer; INL: Inner Nuclear Layer; ONL: Outer Nuclear Layer. *P < 0.05, **P < 0.01.

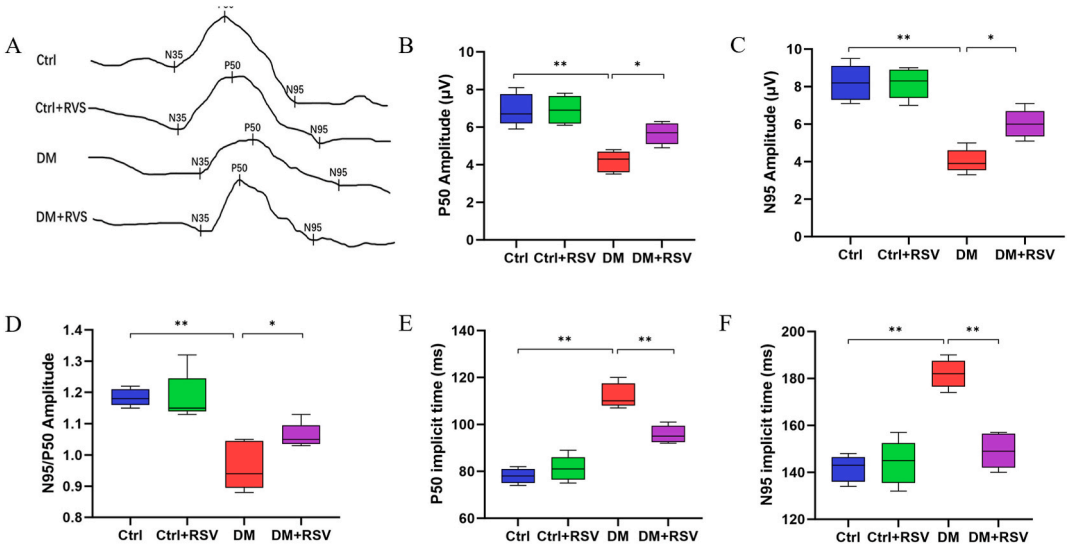

Fig. 2. Pattern ERG responses in the Ctrl, Ctrl + RSV, DM, and DM + RSV groups. (A) The typical presentations of electroretinograms in mice from different groups. (B) The P50 response's average contrast amplitude across the four groups. (C) The four groups' average contrast amplitude of the N95 response. (D) The proportion between the four groups' absolute N95 and P50 wave amplitude values. (E) The P50 response's average contrast implicit time across the four groups. (F) The group average contrast implicit time of the N95 reaction. For comparing several groups (n = 5), the nonparametric Kruskal-Wallis test was employed and then the Mann-Whitney test. The values represent the means ± SD deviation of separate studies. **P < 0.01 and *P < 0.05.

3.3. Effect of RSV on retinal ganglion cell (RGC) apoptosis in diabetic retinas

For signal transduction to occur, a functioning cell mass must be maintained. Reduced cell population-induced dysfunction is thought to play a major role in the etiology of a number of metabolic disorders. We looked into the function of RGCs, which were shown to be much less in the retinas of diabetic mice than in the retinas of normal mice, as shown in Fig. 2, and RSV corrected this impact. We used TUNEL assays to measure apoptosis in order to evaluate the impact of RSV on RGCs. TUNEL labeling is used to identify DNA damage, as seen in Fig. 3A. In the retinas of normal control mice and those treated with RSV alone (10 mg/kg/day), no TUNEL-positive cells were observed. In contrast, the retinas of diabetic mice showed a substantial increase in TUNEL-positive cells in many layers (GCL: 11,435.23 ± 443.18, shown in Fig. 3B; Inner Nuclear Layer, INL: 10,765 ± 486.23, shown in Fig. 3C; and Outer Nuclear Layer, ONL: 10,234.34 ± 464.15, shown in Fig. 3D). TUNEL-positive cells in the ONL, INL, and GCL of diabetic mice retinas were dramatically decreased by 10 mg/kg/day of RSV therapy (ONL: 10,234.34 ± 464.15; INL: 10,765 ± 486.23; and GCL: 11,435.23 ± 443.18). Consequently, the number of TUNEL-positive cells was significantly reduced by around 45% as a consequence of RSV therapy, indicating that diabetes induced apoptosis of RGCs, and RSV mitigated apoptosis in the retinas.

3.4. Impact of RSV on Nrf2 and SLC7A11 protein expression in retinal tissues

In the retinal tissues of mice belonging to various groups, we examined the protein expression levels and localization of Nrf2 and SLC7A11. Fig. 4A illustrates the limited and consistent expression of Nrf2 in the retinas of the normal control group, which was localized in several layers, particularly the cytoplasm of RGCs. Meanwhile, SLC7A11 was primarily expressed in the choroid layer, with less expression in the retinal nerve layer. In the Ctrl + RSV group, Nrf2 in the ganglion cells was slightly activated (Fig. 4B), and SLC7A11 expression in the choroid increased slightly compared to normal levels (Fig. 4C). We found a substantial reduction in Nrf2 and SLC7A11 expression in the DM group. On the other hand, Nrf2 was considerably activated and SLC7A11 expression was dramatically upregulated in the DM + RSV treatment group. In the retinas of the RSV treatment group, Nrf2 and SLC7A11 expression rose 4.60 and 4.13 folds, respectively, in comparison to the DM group.

RSV Regulation of the Nrf2 Signaling Pathway Mitigates Oxidative Stress-Induced Damage in HG-Induced Retinal Ganglion Cells (RGCs)

We first evaluated the MDA and SOD activity in RGCs to clarify the effect of RSV on HG-induced oxidative damage in RGCs. The MDA content of the HG group was significantly higher than that of the normal control group, as shown by the experimental results (Fig. 5A). In contrast to the HG group, the MDA content was much lower in the RSV therapy group. SOD activity was much lower in the

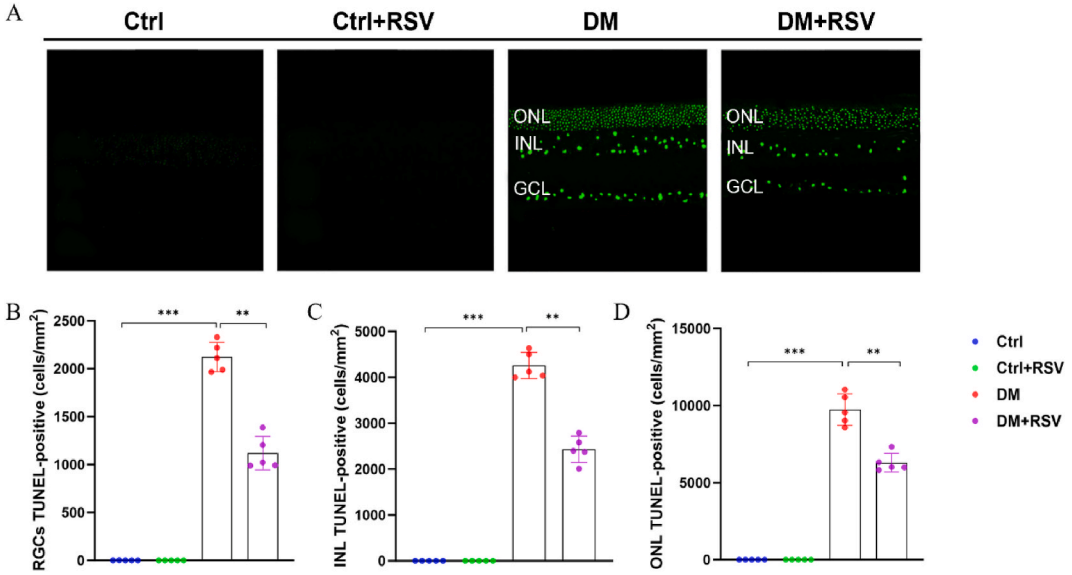

Fig. 3. The impact of RSV on RGC apoptosis as measured by TUNEL tests. (A) A comparison of the TUNEL-positive apoptosis of RGCs across several groups. Scale bar: 100 μm. (B) A comparison of the quantity of apoptotic cells in various RGC populations. In comparison to the normal control group, the diabetic (DM) group had a significantly higher rate of RGC apoptosis, whereas there is a discernible increase in the number of apoptotic RGCs after treatment with RSV. (C) Apoptotic cell numbers in different groups of inner nuclear layer (INL). Similar to the pattern observed in RGC apoptosis, there is a significant increase in apoptotic INL cells in the model group of mice. In comparison to the initial condition, there is a decrease in the quantity of apoptotic cells in the DM + RSV group. (D) Apoptotic cell numbers in different groups of outer nuclear layer (ONL). In the mouse model group, there is a notable rise in apoptotic INL cells, which is consistent with the pattern of RGC apoptosis. On the other hand, compared to the prior condition, there is a reduction in the quantity of apoptotic cells in the DM + RSV group. The values represent the means ± standard deviation of separate studies. For multiple-group comparison, the nonparametric Kruskal-Wallis test and the Mann-Whitney test were employed (n = 5). GCL: Ganglion Cell Layer; INL: Inner Nuclear Layer; ONL: Outer Nuclear Layer. *P < 0.05, **P < 0.01.

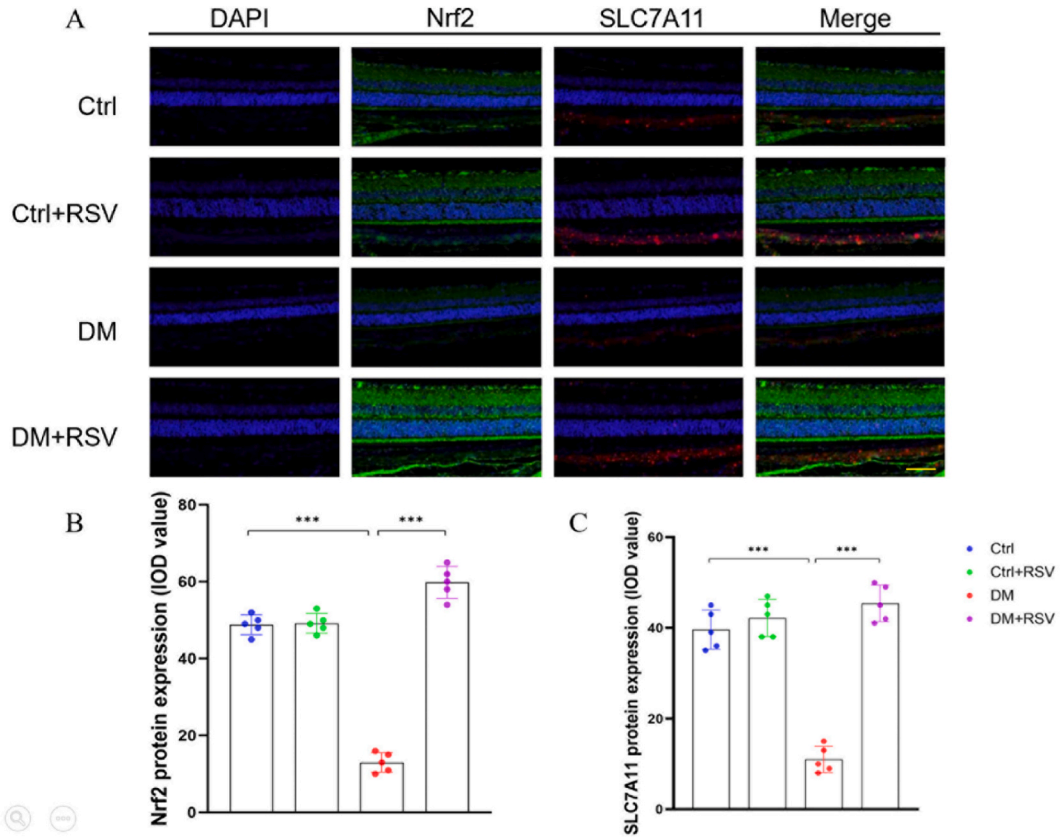

Fig. 4. The protein expression levels and localization of Nrf2 and SLC7A11 in the retinal tissues of mice from different groups. (A) Retinal tissues from different groups were immunofluorescence stained, and slices were counterstained with DAPI (blue) to show the expression and location of Nrf2 (green) and SLC7A11 (red). The photos were 400 times magnified. 100 μm is the scale bar. (B) The fluorescence of the Nrf2 protein in the retina was quantified. (C) A quantitative examination of the retina's SLC7A11 protein fluorescence was also done. The information is shown as mean ± SD (n = 5). For multiple-group comparison, the nonparametric Kruskal-Wallis test and the Mann-Whitney test were employed (n = 5). *P < 0.05, **P < 0.01.

HG group when compared to the normal group, but it was significantly higher in the RSV therapy group when compared to the model group (Fig. 5B). Additionally, Nrf2, HO-1, and SLC7A11 were among the molecules linked to the Nrf2 signaling pathway whose expression was assessed by qRT-PCR. The Nrf2, HO-1, and SLC7A11 expression levels were considerably lower in the HG group than in the normal control group, but they were significantly higher in the RSV treatment group, according to the data (Fig. 5C–E). Furthermore, Nrf2 signaling pathway molecule protein expression was confirmed by western blotting. The findings of the experiment (Fig. 6A) showed that Nrf2 deletion dramatically increased the production of the apoptotic protein Caspase3 in HG-induced RGCs (Fig. 6B), whereas Nrf2 and HO-1 expression considerably reduced. Proteins linked to apoptosis continued to express themselves even after receiving further RSV injections. All of these findings point to the importance of the Nrf2 signaling pathway in the HG-induced death of RGCs, and the ability of RSV to control the expression of proteins involved in the Nrf2 signaling pathway.

4. Discussion

In the neurodegenerative process of diabetic retinopathy, RGCs, photoreceptor cells, and Müller glial cells undergo degenerative changes [14]. Xiao et al. [15] demonstrated that RSV significantly reduces RGC apoptosis in STZ-induced diabetic mice, decreases caspase-3 expression, and maintains inner retinal thickness. This is explained by the fact that RSV inhibits the activation of calcium/calmodulin-dependent protein kinase II. Seong et al. [16] confirmed that after ischemia/reperfusion (I/R) injury, human epidermal growth factor receptor 2 (ErbB2) expression was upregulated, and the GCL showed an increase in apoptosis. RSV treatment prevented I/R-induced ganglion cell death while concurrently lowering apoptosis and downregulating the expression of the ErbB2 protein in the retina. RSV showed its effect on apoptosis in later in vitro models by adjusting the phosphorylation and expression levels of ErbB2 and mouse double minute 2 homolog (MDM2). These results show that, in the setting of ischemia damage, RSV efficiently inhibits GCL-specific apoptosis via downregulating ErbB2. Although the protective effects of RSV on RGCs are supported by the aforementioned studies, the underlying protective mechanisms still require further research and evidence. We found that RSV dramatically lowers the apoptosis of diabetic retinal ganglion cells in our investigation. This protective effect is achieved by inducing

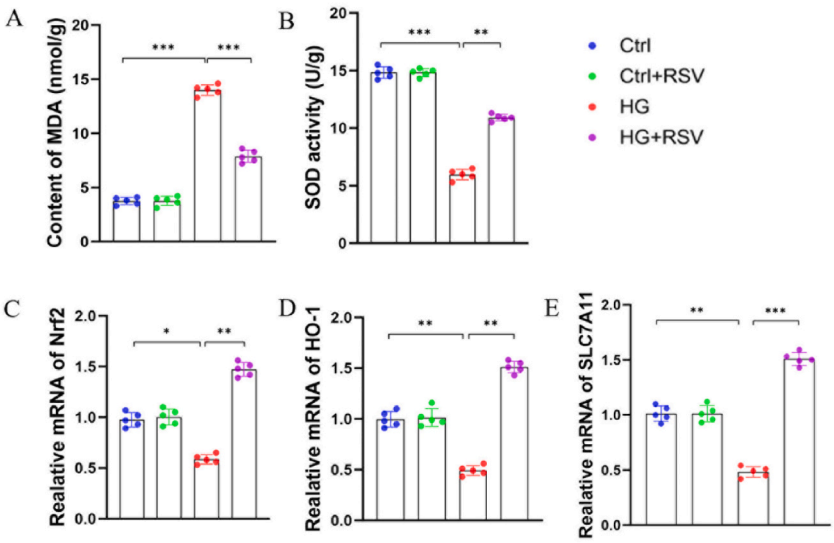

Fig. 5. The impact of RSV on HG-induced oxidative damage in RGCs. (A) The content of MDA in RGCs within different groups. We found an increased MDA level in HG group, and decreased in RSV treatment group. (B) The SOD activity of RGCs in different groups. With the effect of HG, the SOD activity significantly decreased but increased in RSV group. (C) Nrf2 mRNA levels in RGCs following exposure to HG and RSV. (D) The HO-1 mRNA level in RGCs following exposure to HG and RSV. (E) The mRNA level of SLC7A11 in RGCs after HG and RSV exposure. (unpaired *t*-test, n = 5). *P < 0.05, **P < 0.01.

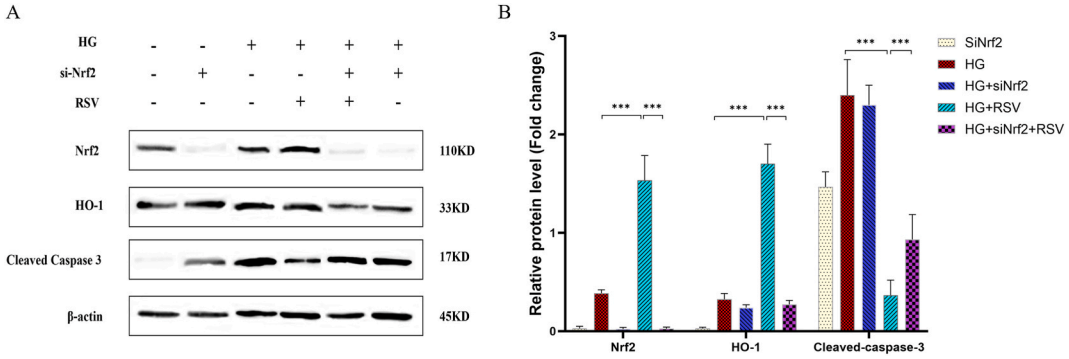

Fig. 6. The Western blotting results and measurement of Nrf2, HO-1, and cleaved caspase 3 in RGC cells following HG exposure and Nrf2 knockdown (n = 3, two-way ANOVA, Tukey's test). (A) The image of the Western blotting in various groups. (B) A comparison of the RGCs in various groups' quantification using Nrf2, HO-1, and cleaved caspase 3. For multiple-group comparison (n = 3), the nonparametric Kruskal-Wallis test and the Mann-Whitney test were employed. **P < 0.01 and *P < 0.05.

high expression of Nrf2 signaling molecules and activating the HO-1 signaling pathway, resulting in a decrease in caspase-3 linked to apoptosis expression and providing protection against oxidative stress-induced damage to RGCs.

The purpose of this work is to look at how RSV protects diabetic mice's retinal gingicle cells. Histological analyses using TUNEL and H&E staining showed that the diabetic mice's retinas had more regular structures in each layer after receiving RSV therapy. Of particular note was the increase in the quantity and nuclear density of RGCs in comparison to the model group. These findings suggest that RSV may mitigate RGC apoptosis and offer protective effects on retinal tissue integrity. Pattern ERG serves as a non-invasive tool for assessing retinal function, primarily reflecting the functionality of the inner retinal layers, notably RGCs, aiding in the diagnosis of RGC damage [17]. Relying only on one sign to measure damage to RGCs may have drawbacks because the P50 and N95 waves in Pattern ERG have different sources, with the N95 wave perhaps originating from the retinal GCL and the P50 wave's origin being unknown [18]. To mitigate this, we employed the diagnostic criterion of N95/P50 < 1.1, where the ratio of the absolute values of N95 and P50 wave amplitudes is less than 1.1. This approach helps to avoid issues arising from comparing N95 wave amplitudes when they are too small or absent. Pattern ERG represents the aggregate of electrical responses from RGC, with its amplitude closely tied to the number of ganglion cells present [19]. Even a slight degeneration or loss of ganglion cells can lead to decline in Pattern ERG amplitude, worsening with the disease progression. Our study results indicate a significant enhancement in Pattern ERG amplitude following RSV treatment in mice compared to the model group, indicative a positive impact on both the quantity and functionality of retinal ganglion

cells. Hence, we posit that RSV exerts a protective influence on diabetic retinal ganglion cells, primarily by mitigating RGC apoptosis and enhancing ganglion cell function.

When physiological circumstances are normal, Nrf2, a transcription factor that is susceptible to oxidative stress, usually stays inactive in the cytoplasm where it connects with Keap1 to preserve cellular homeostasis [20–22]. Nrf2 is activated in response to external oxidative stresses, which causes it to separate from Keap1 and go into the nucleus. After entering the nucleus, Nrf2 interacts with the antioxidant response element (ARE) to control the production of genes involved in downstream antioxidant defense, including NAD(P)H Dehydrogenase Quinone 1 (NQO1) and HO-1. These downstream effectors play a vital role in neutralizing excessive ROS, thus preserving the cellular redox balance and providing cellular protection [23–25]. The activation of the Nrf2 pathway stands as a critical antioxidant stress pathway, demonstrating significant neuroprotective effects against oxidative damage in diabetes-related neuropathies. RSV, often referred to as a natural Nrf2 activator, demonstrates a broad range of biological and pharmacological traits, such as anti-inflammatory, antioxidant, and anti-apoptotic effects [26,27]. It's interesting to see how RSV protects diabetic mice's retinas from oxidative damage. Prior research has demonstrated that RSV can stop cerebral ischemia-induced brain damage by activating the Nrf2 pathway [28,29]. Therefore, we postulate that RSV might prevent damage to RGC induced by DM through the upregulation of Nrf2 transcriptional activity and expression. In the retinas of diabetic mice, our study findings show a significant downregulation of Nrf2 expression along with downstream HO-1, corresponding with a noteworthy upregulation of the death protein caspase-3 in RGCs. In contrast, compared to the model group, the RSV treatment group showed a substantial downregulation of caspase-3 expression and an activation of Nrf2 and downstream antioxidant stress genes in mice retinas. Additionally, through rescue experiments, we observed a significant increase in caspase-3 expression following Nrf2 interference. Consequently, we end by turning on the Nrf2 signaling pathway, which allows RSV to protect against RGC apoptosis.

Our results indicate that the effects of RSV are prominently manifested under conditions of elevated glucose levels. The lack of substantial changes between the Ctrl and Ctrl + RSV groups in normoglycemic circumstances supports this conclusion. The absence of discernible effects in the Ctrl + RSV group implies that the mechanism of action of RSV may be particularly attuned to counteracting the oxidative stress and apoptotic pathways that are heightened during hyperglycemic states. This highlights the specificity of resveratrol's protective effects against retinal ganglion cell apoptosis, particularly in the context of diabetic retinopathy. Based solely on our research results, the effects of resveratrol can be explained in several aspects. First, in normal, or normoglycemic, conditions, the cells may not be experiencing the same level of oxidative stress or apoptotic signals that are characteristic of hyperglycemic states. Therefore, the addition of resveratrol, which is known for its antioxidant and anti-apoptotic properties, may not have a significant impact on cells that are not under substantial stress. On the other hand, in the high-glucose scenario, cells are exposed to increased oxidative stress and apoptotic signals. This is where resveratrol seems to exert its effects most prominently. By targeting these specific pathways that are amplified during hyperglycemia, resveratrol can effectively protect against retinal ganglion cell apoptosis. This finding underscores the importance of context when considering the effects of resveratrol. It suggests that its therapeutic potential may be particularly relevant in conditions where oxidative stress and apoptosis are elevated, such as in diabetic retinopathy. Further exploration of the specific molecular pathways through which resveratrol operates under varying glucose conditions could yield valuable insights into its precise mechanisms of action. This could not only enhance our understanding of its role in managing diabetic retinopathy but also aid in the development of more targeted treatment approaches.

5. Conclusion

In summary, RSV demonstrates neuroprotective effects against RGCs oxidative stress induced by DM via increasing Nrf2 expression and the expression of related antioxidant genes. Nrf2/HO-1 signaling pathway activation is the main mechanism by which RSV confers its protective effect on RGCs. This experiment suggests that RSV holds clinical promise as an intervention for diabetic retinal neuropathy, providing insights and evidence for the prevention of DM-induced retinal neuropathy.

CRediT authorship contribution statement

Dongqing Yuan: Writing – original draft, Project administration, Methodology, Investigation, Funding acquisition, Formal analysis, Data curation, Conceptualization. **Yingnan Xu:** Writing – original draft, Project administration, Methodology, Investigation, Formal analysis, Data curation. **Lian Xue:** Writing – review & editing, Investigation, Formal analysis, Data curation. **Weiwei Zhang:** Visualization, Validation, Supervision, Software, Resources. **Liuwei Gu:** Software, Resources, Project administration, Methodology, Conceptualization. **Qinghuai Liu:** Writing – review & editing, Writing – original draft, Supervision, Funding acquisition, Formal analysis, Conceptualization.

Declaration of competing interest

The authors declare that they have no known competing financial interests or personal relationships that could have appeared to influence the work reported in this paper.

Acknowledgments

This study was supported by the National Natural Science Foundation of China (Grant No. 82271100) and the Jiangsu Science and Technology Support Program (Grant No. BE2022805).

Appendix A. Supplementary data

Supplementary data to this article can be found online at https://doi.org/10.1016/j.heliyon.2024.e30786.

References

[1] S. Chaurasia, A.R. Thool, K.K. Ansari, A.I. Saifi, Advancement in understanding diabetic retinopathy: a comprehensive review, Cureus 15 (11) (2023) e49211.
[2] T.E. Tan, T.Y. Wong, Diabetic retinopathy: looking forward to 2030, Front. Endocrinol. 13 (2023) 1077669.
[3] M.Z. Sadikan, N.A. Abdul Nasir, L. Lambuk, R. Mohamud, N.H. Reshidan, E. Low, S.A. Singar, Z.L. Teo, Y.C. Tham, M. Yu, M.L. Chee, T.H. Rim, N. Cheung, M. M. Bikbov, Y.X. Wang, Y. Tang, Y. Lu, I.Y. Wong, D.S.W. Ting, G.S.W. Tan, J.B. Jonas, C. Sabanayagam, T.Y. Wong, C.Y. Cheng, Global prevalence of diabetic retinopathy and projection of burden through 2045: systematic review and meta-analysis, Ophthalmology 128 (11) (2021) 1580–1591.
[4] Q. Kang, C. Yang, Oxidative stress and diabetic retinopathy: molecular mechanisms, pathogenetic role and therapeutic implications, Redox Biol. 37 (2020) 101799.
[5] A.W. Stitt, T.M. Curtis, M. Chen, R.J. Medina, G.J. McKay, A. Jenkins, T.A. Gardiner, T.J. Lyons, H.P. Hammes, R. Simó, N. Lois, The progress in understanding and treatment of diabetic retinopathy, Prog. Retin. Eye Res. 51 (2016) 156–186.
[6] A.S. Mohmad Sabere, I. Iezhitsa, R. Agarwal, Diabetic retinopathy: a comprehensive update on in vivo, in vitro and ex vivo experimental models, BMC Ophthalmol. 23 (1) (2023) 421.
[7] A. Shaito, A.M. Posadino, N. Younes, H. Hasan, S. Halabi, D. Alhababi, A. Al-Mohannadi, W.M. Abdel-Rahman, A.H. Eid, G.K. Nasrallah, G. Pintus, Potential adverse effects of resveratrol: a literature review, Int. J. Mol. Sci. 21 (6) (2020) 2084.
[8] B. Tian, J. Liu, Resveratrol: a review of plant sources, synthesis, stability, modification and food application, J. Sci. Food Agric. 100 (4) (2020) 1392–1404.
[9] I. Ahmad, M. Hoda, Attenuation of diabetic retinopathy and neuropathy by resveratrol: review on its molecular mechanisms of action, Life Sci. 245 (2020) 117350.
[10] Z. Xie, Q. Ying, H. Luo, M. Qin, Y. Pang, H. Hu, J. Zhong, Y. Song, Z. Zhang, X. Zhang, Resveratrol alleviates retinal ischemia-reperfusion injury by inhibiting the NLRP3/gasdermin D/Caspase-1/Interleukin-1β pyroptosis pathway, Invest. Ophthalmol. Vis. Sci. 64 (15) (2023) 28.
[11] W. Zhang, H. Yu, Q. Lin, X. Liu, Y. Cheng, B. Deng, Anti-inflammatory effect of resveratrol attenuates the severity of diabetic neuropathy by activating the Nrf2 pathway, Aging (Albany NY) 13 (7) (2021) 10659–10671.
[12] H. You, H. Li, W. Gou, lncRNA HOTAIR promotes ROS generation and NLRP3 inflammasome activation by inhibiting Nrf2 in diabetic retinopathy, Medicine (Baltim.) 102 (37) (2023) e35155.
[13] G. Xu, X. Zhao, J. Fu, X. Wang, Resveratrol increase myocardial Nrf2 expression in type 2 diabetic rats and alleviate myocardial ischemia/reperfusion injury (MIRI), Ann. Palliat. Med. 8 (5) (2019) 565–575.
[14] S. Shi, C. Ding, S. Zhu, F. Xia, S.E. Buscho, S. Li, M. Motamedi, H. Liu, W. Zhang, PERK inhibition suppresses neovascularization and protects neurons during ischemia-induced retinopathy, Invest. Ophthalmol. Vis. Sci. 64 (11) (2023) 17.
[15] K. Xiao, X.H. Ma, Z. Zhong, Y. Zhao, X.H. Chen, X.F. Sun, Low-dose trans-resveratrol ameliorates diabetes-induced retinal ganglion cell degeneration via TyrRS/c-jun pathway, Invest. Ophthalmol. Vis. Sci. 64 (7) (2023) 2.
[16] H. Seong, J.Y. Jeong, J. Ryu, J. Park, Y.S. Han, H.K. Cho, S.J. Kim, J.M. Park, S.S. Kang, S.W. Seo, Resveratrol prevents hypoxia-induced retinal ganglion cell death related with ErbB2, Int. J. Ophthalmol. 15 (3) (2022 Mar 18) 394–400.
[17] T.H. Chou, J. Toft-Nielsen, V. Porciatti, High-throughput binocular pattern electroretinograms in the mouse, Methods Mol. Biol. 2708 (2023) 147–153.
[18] Habjan M. Sustar, J. Brecelj, M. Hawlina, Analysis of the slope between P50 and N95 waves of the large field pattern electroretinogram as an additional indicator of ganglion cell dysfunction, Doc. Ophthalmol. 147 (2) (2023) 77–88.
[19] D. Orshan, A. Tirsi, H. Sheha, V. Gliagias, J. Tsai, S.C. Park, S.A. Obstbaum, C. Tello, Structure-function models for estimating retinal ganglion cell count using steady-state pattern electroretinography and optical coherence tomography in glaucoma suspects and preperimetric glaucoma: an electrophysiological pilot study, Doc. Ophthalmol. 145 (3) (2022) 221–235.
[20] M.F. Balaha, A.A. Alamer, R.M. Aldossari, A.H. Aodah, A.I. Helal, A.M. Kabel, Amentoflavone mitigates cyclophosphamide-induced pulmonary toxicity: involvement of -SIRT-1/Nrf2/Keap1 Axis, JAK-2/STAT-3 signaling, and apoptosis, Medicina (Kaunas) 59 (12) (2023) 2119.
[21] L. Xiong, T. Lin, X. Yue, S. Zhang, X. Liu, F. Chen, S. Zhang, W. Guan, Maternal selenium-enriched yeast supplementation in sows enhances offspring growth and antioxidant status through the nrf2/keap1 pathway, Antioxidants 12 (12) (2023) 2064.
[22] L. Yan, X. Han, M. Zhang, H. Kou, H. Liu, T. Cheng, Melatonin exerts neuroprotective effects in mice with spinal cord injury by activating the Nrf2/Keap1 signaling pathway via the MT2 receptor, Exp. Ther. Med. 27 (1) (2023) 37.
[23] K. Yan, L. Li, S. Ye, Q. Xu, L. Ding, Sevoflurane alleviates oxygen-glucose deprivation/reoxygenation-induced damage in HT22 cells by activating the Keap1/Nrf2/ARE pathway to inhibit oxidative stress, Int. J. Neurosci. (2023) 1–8.
[24] H.M. Assiry, A.R. Hamed, G.A. Mohamed, S.R.M. Ibrahim, A.E. Koshak, A.M. Malebari, S.A. Fadil, H.M. Abdallah, Acetyl barlerin from Barleria trispinosa induces chemopreventive NQO1 and attenuates LPS-induced inflammation: in vitro and molecular dynamic studies, J. Biomol. Struct. Dyn. (2023) 1–12.
[25] A. Khan, F. Wang, B. Shal, A.U. Khan, S.S. Zahra, I.U. Haq, S. Khan, K.R. Rengasamy, Anti-neuropathic pain activity of Ajugarin-I via activation of Nrf2 signaling and inhibition of TRPV1/TRPM8 nociceptors in STZ-induced diabetic neuropathy, Pharmacol. Res. 183 (2022) 106392.
[26] K. Xu, X. Chang, X. Bai, H.B. Liu, X.B. Chen, H.P. Chen, Y.H. Liu, Activation of Nrf2 inhibits ferroptosis and protects against oxaliplatin-induced ototoxicity, Biomed. Pharmacother. 165 (2023) 115248.
[27] Z. Xu, X. Sun, B. Ding, M. Zi, Y. Ma, Resveratrol attenuated high intensity exercise training-induced inflammation and ferroptosis via Nrf2/FTH1/GPX4 pathway in intestine of mice, Turk. J. Med. Sci. 53 (2) (2023) 446–454.
[28] C. Li, Z. Wu, H. Xue, Q. Gao, Y. Zhang, C. Wang, P. Zhao, Ferroptosis contributes to hypoxic-ischemic brain injury in neonatal rats: role of the SIRT1/Nrf2/GPx4 signaling pathway, CNS Neurosci. Ther. 28 (12) (2022) 2268–2280.
[29] J. Liu, J. Chen, J. Zhang, Y. Fan, S. Zhao, B. Wang, P. Wang, Mechanism of resveratrol improving ischemia-reperfusion injury by regulating microglial function through microRNA-450b-5p/KEAP1/nrf2 pathway, Mol. Biotechnol. 65 (9) (2023) 1498–1507.